

1 A Expanded Related Work

2 A.1 Causal inference for binary treatments

3 Much recent work [1, 2, 3, 4] in causal inference focuses on the scenario with binary treatments to
4 estimate causal effects that are defined as the expected difference between the treated and control
5 outcomes, where the selection bias problem has been extensively studied.

6 In observational data, treatments are typically assigned according to the covariates associated with
7 each unit, resulting in unbalanced covariate distributions among subpopulations that received different
8 treatments, which is known as *selection bias* [5]. It is an important problem on how to alleviate the
9 imbalance which can lead to an unreliable inference. In the binary treatment setting, one approach to
10 the problem of selection bias is re-weighting the units in observational data to balance the treated
11 and control groups [6, 3, 4]. Most of these re-weighting methods are based on the propensity score
12 proposed in [6], which is defined as the probability of treatment assignment conditional on observed
13 covariates. For example, inverse probability of treatment weighting (IPTW) [7] defines a unit's
14 sample weight as the inverse of the probability of receiving the treatment that the unit actually
15 received, and demonstrates that the distribution of covariates in treated and control groups could be
16 balanced using this weight. Hassanpour and Greiner [3] use the importance sampling technique to
17 propose a context-aware weight, which is defined on the basis of the propensity score and emphasizes
18 those units that are important for counterfactual inference. Extended from the standard propensity
19 score, the generalized propensity score (GPS) [8], defined as the conditional density of the treatments
20 conditional on observed covariates, has a similar balancing property in alleviating the selection bias
21 in the continuous treatment setting. Although the methods [9, 10] based on the GPS have some
22 attractive theoretical features, they may suffer from the drawback that the GPS is far more difficult to
23 estimate accurately compared to the standard propensity score [11].

24 The Integral Probability Metric (IPM) that measures the distance between distributions has been
25 also exploited to mitigate selection bias in some neural network-based methods for causal inference
26 [1, 12, 3, 4]. For example, Shalit et al. [1] propose an algorithm that learns a balanced representation
27 of covariates such that the distributions of treated and control groups look similar, i.e., with reduced
28 IPM distance between these two groups. After that, a linear ridge-regression model is fitted using the
29 factual (observed) distribution on top of learned representations, which bounds the relative error when
30 using the distribution with reverse treatment assignment (counterfactual loss). Unlike regression-
31 based models [1], Li and Fu [12] design a matching estimator based on the learned low-dimensional
32 balanced and nonlinear representations (BNR) for observational data, incorporating a Maximum
33 Mean Discrepancy (MMD) criterion into the model. Yao et al. [2] not only balance the distributions
34 of treated and control groups to reduce selection bias but also preserve the local similarity among
35 units, which provides meaningful constraints on estimating causal effects. However, these methods
36 for adjusting selection bias for binary (also discrete) treatments cannot be easily extended to the
37 continuous treatment settings since there may be uncountably many groups that received different
38 treatments.

39 A.2 Connection between causal inference and domain adaptation

40 Shalit et al. [1] have found a strong connection between causal inference and domain adaptation. Es-
41 timating the average treatment effect in the binary treatment setting requires predicting counterfactual
42 outcomes over a different "target" (counterfactual) data distribution based on the "source" (observed)
43 one, which has similarities with domain adaptation methods that focus on transferring knowledge
44 between discrete domains [13, 14, 15]. Shalit et al. [1] employ the IPM distance between treated and
45 control groups to bound the generalization error of estimating causal effects in the binary treatment
46 setting, similar to the generalization bound in domain adaptation given by [16]. In the continuous
47 treatment setting, causal inference is highly related to the continuously indexed domain adaptation
48 [17, 18, 19], which focuses on the scenario where the target domain usually come in a continually
49 evolving manner, such as from day to night. From a domain adaptation perspective, estimating
50 ADRF ($T = t$) requires predicting counterfactual outcomes (Y^t) over a continually evolving "target"
51 (counterfactual) distribution $p(X, Y^t|T = s)$ ($s \in [0, 1]$ and $s \neq t$) based on the "source" (observed)
52 distribution $p(X, Y^t|T = t)$. We bound the generalization error of estimating ADRF by an IPM
53 term defined on observed and counterfactual distributions. However, it is impractical to calculate this
54 IPM term since potentially infinite counterfactual distributions may exist in a continuous treatment

55 scenario. Following [18], we make an assumption that the covariates distributions of subpopulations
 56 receiving different treatments smoothly shift, under which we provide a discretized approximation of
 57 this IPM term and propose an algorithm to calculate it in practice.

58 A.3 Theoretical connection between ADMIT and causal inference for binary treatments

59 The theoretical part of our work is built on multiple work on causal inference for binary treatments,
 60 such as [1, 3, 4]. Shalit et al. [1] prove that expected Precision in Estimation of Heterogeneous Effect
 61 (PEHE) loss is upper bounded by the sum of the expected factual loss and expected counterfactual
 62 loss when the squared loss is adopted in these two losses. After that, on the basis of the theoretical
 63 results related to domain adaptation [13], Shalit et al. [1] bound the counterfactual loss by the factual
 64 loss and an IPM, which is adopted in our work. Hassanpour et al. [3] propose context-aware weights
 65 that incorporate the valuable context information of each instance, built on top of a representation
 66 learning module in [1]. While the context-aware weights are obtained based on the estimation of the
 67 propensity score, Johansson et al. [4] propose adaptable sampling weights to balance the treated and
 68 control groups, which is adopted in our work.

69 Our ADRF error upper bound has similarities with generalization bounds in [1, 4], but with significant
 70 differences due to the continuity of the treatment. Continuous treatments induce uncountably many
 71 potential outcomes per unit, which leads to a more complex selection bias problem than binary
 72 treatments. The potentially infinite number of counterfactual distributions is the main challenge
 73 since the number of samples for each subpopulation is not enough to estimate the IPM in practice.
 74 Therefore, we introduce an assumption to constrain differences in the distributions of subpopulations
 75 receiving different treatments. Based on this assumption, we provide the approximation of the IPM
 76 term to make it operational and derive an ADRF error upper bound using the IPM term.

77 B Proofs

78 **Theorem 1.** *Let L be the squared loss function, i.e., $L(y, y') = (y - y')^2$. For hypotheses f_t
 79 of individual dose-response function $\mu(t, \cdot)$ with marginal loss $\epsilon(f_t) = \mathbb{E}[l_{f_t}(X)]$, there exists a
 80 constant $\sigma_{min} \geq 0$, such that,*

$$\text{EMSE}(\mu, \hat{\mu}) \leq \mathbb{E}_T[\epsilon(f_t)] - \sigma_{min}. \quad (1)$$

81

82 *Proof.* Let u, v be two arbitrary random variables with limited expected values, i.e., $\mathbb{E}[u], \mathbb{E}[v] < \infty$.

83 Based on the Cauchy–Schwarz inequality, the following inequality holds,

$$(\mathbb{E}[uv])^2 \leq \mathbb{E}[u^2]\mathbb{E}[v^2]. \quad (2)$$

84 By replacing u and v with $f_t(X) - \mu(t, X)$ and 1 in inequality (2), respectively, we get

$$(\mathbb{E}[f_t(X)] - \mathbb{E}[\mu(t, X)])^2 \leq \mathbb{E}[(f_t(X) - \mu(t, X))^2]. \quad (3)$$

85 Based on the bias-variance decomposition of the squared loss, the marginal loss $\epsilon(f_t)$ could be
 86 decomposed as:

$$\epsilon(f_t) = \mathbb{E}[(Y^t - \mu(t, X))^2] + \mathbb{E}[(f_t(X) - \mu(t, X))^2]. \quad (4)$$

87 The term $\mathbb{E}[(Y^t - \mu(t, X))^2]$ is a constant determined by the data generation process, denoted by
 88 $\sigma_t(Y)$. Combining inequality (3) and equality (4), we get

$$(\hat{\mu}(t) - \mu(t))^2 \leq \epsilon(f_t) - \sigma_t(Y), \quad (5)$$

89 where $\mu(t) = \mathbb{E}[\mu(t, X)]$ and $\hat{\mu}(t) = \mathbb{E}[f_t(X)]$. Let $\sigma_{min} = \min\{\sigma_t(Y)\} \forall t \in [0, 1]$, and take
 90 expectations on both sides, we have our result. □

91

92 **Lemma 1.** *Let \mathcal{G} be a family of functions $l : \mathcal{X} \rightarrow \mathcal{R}$. Assume the per-unit expected loss function
 93 $L(f, f') \in \mathcal{G}$ for all $f, f' \in \mathcal{H}$. Then for any $s \in [0, 1]$ and $s \neq t$, we have:*

$$\epsilon(f_t|T = s) \leq \epsilon_w(f_t|T = t) + \text{IPM}_{\mathcal{G}}(p_s, p_t^w). \quad (6)$$

94

95 *Proof.* By definitions of the *conditional loss* and $\text{IPM}_{\mathcal{G}}$, the following holds,

$$\begin{aligned} & \epsilon(f_t|T = s) - \epsilon_w(f_t|T = t) \\ &= \mathbb{E}_{X|T}[l_f(x)|T = s] - \mathbb{E}_{X|T}[w(x)l_f(X)|T = t] \\ &\leq \left| \int l_f(x)(p_s(x) - p_t^w(x))dx \right| \\ &\leq \sup_{g \in \mathcal{G}} \left| \int g(x)(p_s(x) - p_t^w(x))dx \right| \\ &= \text{IPM}_{\mathcal{G}}(p_t^w, p_s). \end{aligned}$$

96 **Theorem 2.** Let $\text{IPM}_{max} = \max_{s \in [0,1]} \{\text{IPM}_{\mathcal{G}}(p_s, p_t^w)\}$. The following holds under the conditions
97 of Lemma 1,

$$\epsilon(f_t) \leq \epsilon_w(f_t|T = t) + \text{IPM}_{max}. \quad (7)$$

98

99 *Proof.* By the law of iterated expectation and Lemma 1, we have our result:

$$\begin{aligned} \epsilon(f_t) &= \int \epsilon(f_t|T = s)p(s)ds \\ &\leq \int (\epsilon_w(f_t|T = t) + \text{IPM}_{max})p(s)ds \\ &= \epsilon_w(f_t|T = t) + \text{IPM}_{max}. \end{aligned}$$

100 **Assumption 3.** Let p_{t_1} and p_{t_2} denote the conditional probability densities of subpopulations that
101 received treatment t_1 and t_2 , respectively. We assume that there is a constant α such that the following
102 inequality holds $\forall t_1, t_2 \in [0, 1]$:

$$\text{IPM}_{\mathcal{G}}(p_{t_1}, p_{t_2}) \leq \alpha |t_1 - t_2|. \quad (8)$$

103

104 We bound the difference between the IPM_{max} and its discretization under Assumption 3 that the
105 probability distributions of subpopulations that received different treatments shift smoothly.

106 **Lemma 2.** Suppose we have n i.i.d. sample of units, and the i th unit received a treatment $t_i \sim p(t)$.
107 We assume Assumption 3 holds for a constant α . Then the following holds,

$$\text{IPM}_{max} \leq \max_{i \in \{1, \dots, n\}} \{\text{IPM}_{\mathcal{G}}(p_{t_i}, p_t^w)\} + O_p\left(\frac{\alpha}{\sqrt[3]{n}}\right). \quad (9)$$

108

109 *Proof.* Without loss of generality, assume $t_1 \leq t_2 \leq \dots \leq t_n$. Consider a sequence of random
110 variables: $\{L_n\}_{n=1,2,\dots}$, where $L_n = \max_{i \in \{0,1,2,\dots,n\}} (|t_{i+1} - t_i|)$ ($t_0 = 0, t_{n+1} = 1$), we first
111 prove that L_n converges in probability to zero, whose rate of convergence is at least $n^{-1/3}$, i.e.,
112 $L_n = O_p\left(\frac{1}{\sqrt[3]{n}}\right)$.

113 Let $\beta = p_{max}(t)/p_{min}(t)$, where $p_{min}(t)$ and $p_{max}(t)$ are the minimum and maximum probability
114 of $p(t)$, respectively. Suppose I_i is the interval $[d_{i-1}, d_i]$, where each I_i satisfies $\int_{t \in I_i} p(t)dt = \frac{1}{m}$
115 ($d_0 = 0$ and $d_m = 1$), for $i = 1, 2, \dots, m$. Let A denote the event $\exists i \in \{1, \dots, m\}, \forall j \in$
116 $\{1, \dots, n\}, t_j \notin I_i$. Then the following holds,

$$\begin{aligned} P(L_n \geq \frac{2\beta}{m}) &\leq P(A) \\ &= 1 - \frac{\binom{n-1}{m-1}}{\binom{n+m-1}{m-1}} \\ &= 1 - \frac{(n-1)!n!}{(n-m)!(n+m-1)!} \\ &= 1 - \frac{(n-m+1) \times (n-m+2) \times \dots \times (n-1)}{(n+1) \times (n+2) \times \dots \times (n+m-1)} \\ &< 1 - \left(\frac{n-m}{n}\right)^m. \end{aligned}$$

117 For any $\varsigma > 0$, there exist numbers $1 < M = 2\beta < \infty$ and $N = (\frac{1}{-\log(1-\varsigma)})^3$ such that

$$\begin{aligned} P(L_n \geq \frac{M}{\sqrt[3]{n}}) &< 1 - (1 - \frac{\sqrt[3]{n}}{n})^{\sqrt[3]{n}} \\ &= 1 - (1 - \frac{\sqrt[3]{n}}{n})^{\frac{n}{\sqrt[3]{n}} \times (\frac{\sqrt[3]{n}}{n})^2} \\ &\simeq 1 - e^{-\frac{1}{\sqrt[3]{n}}} \\ &< \varsigma \end{aligned}$$

118 for any $n > N$. Therefore, $L_n = O_p(\frac{1}{\sqrt[3]{n}})$. Under Assumption 3, $\forall i \in \{0, 1, \dots, n, n+1\}$,
119 $\forall s \in [t_i, t_{i+1}]$, the following holds,

$$\begin{aligned} \text{IPM}_{\mathcal{G}}(p_s, p_t^w) &\leq \text{IPM}_{\mathcal{G}}(p_{t_i}, p_t^w) + \text{IPM}_{\mathcal{G}}(p_{t_i}, p_s) \\ &\leq \text{IPM}_{\mathcal{G}}(p_{t_i}, p_t^w) + O_p(\frac{\alpha}{\sqrt[3]{n}}). \end{aligned}$$

120 By the definition of IPM_{max} , we have our result. \square

121 **Lemma 3.** Let $p_{\Delta s} = P_{X|T}(x|t \in [s, s + \delta])$ ($0 < \delta < 1$) denote the conditional density of
122 covariates when $t \in [s, s + \delta]$. Then the following holds under Assumption 3,

$$\text{IPM}_{\mathcal{G}}(p_s, p_t^w) \leq \text{IPM}_{\mathcal{G}}(p_{\Delta s}, p_t^w) + \alpha\delta. \quad (10)$$

123

124 *Proof.* Due to the triangle inequality for the *Integral Probability Metric*,

$$\text{IPM}_{\mathcal{G}}(p_s, p_t^w) \leq \text{IPM}_{\mathcal{G}}(p_{\Delta s}, p_t^w) + \text{IPM}_{\mathcal{G}}(p_{\Delta s}, p_s).$$

125 By the definition of the $\text{IPM}_{\mathcal{G}}$, the following holds,

$$\begin{aligned} &\text{IPM}_{\mathcal{G}}(p_{\Delta s}, p_s) \\ &= \sup_{l \in \mathcal{G}} \left| \int_x l(x) p_s(x) d(x) - \int_s^{s+\delta} p(t|t \in [s, s+\delta]) dt \int_x l(x) p_t(x) dx \right| \\ &= \sup_{l \in \mathcal{G}} \left| \int_s^{s+\delta t} p(t|t \in [s, s+\delta]) dt \int_x l(x) (p_s(x) - p_t(x)) dx \right| \\ &\leq \sup_{l \in \mathcal{G}} \int_s^{s+\delta t} p(t|t \in [s, s+\delta]) dt \left| \int_x l(x) (p_s(x) - p_t(x)) dx \right| \\ &\leq \alpha\delta. \end{aligned}$$

126 Therefore, we have our result. \square

127 **Theorem 3.** Suppose we have n i.i.d. sample of units, and the i th unit received a treatment t_i . Let
128 $\text{IPM}_{\Delta max} = \max_{i \in \{1, \dots, n\}} \{\text{IPM}_{\mathcal{G}}(p_{\Delta t_i}, p_t^w)\}$. We assume Assumption 3 holds for a constant α .
129 Then, for a neighborhood size $0 < \delta < 1$ we have,

$$\epsilon(f_t) \leq \epsilon_w(f_t|T = t) + \text{IPM}_{\Delta max} + O_p(\frac{\alpha}{\sqrt[3]{n}}) + \alpha\delta. \quad (11)$$

130

131 *Proof.* Following Lemma 2 and Lemma 3, we could proof Theorem 3. \square

132 **Property 1.** The minimum α that meets the conditions of Assumption 3 is

$$\alpha_{min} = \max_{s \in [0,1]} \left\{ \lim_{\delta \rightarrow 0} \frac{\text{IPM}(p_s, p_{s+\delta})}{\delta} \right\}. \quad (12)$$

133 *Proof.* Let $t_1 < t_2$ denote two arbitrary variables in $[0, 1]$. We divide $[t_1, t_2]$ into n intervals, each of
 134 length $\eta = \frac{t_2 - t_1}{n}$.

According to the triangle inequality for the Integral Probability Metric, we can get,

$$\text{IPM}(t_1, t_2) \leq \sum_{i=0}^{n-1} \text{IPM}(t_1 + \eta i, t_1 + \eta(i+1)).$$

135 Let $\alpha(t)$ denote $\lim_{\delta \rightarrow 0} \frac{\text{IPM}(p_s, p_{s+\delta})}{\delta}$, then we have,

$$\int_{t_1}^{t_2} \alpha(t) dt = \lim_{n \rightarrow \infty} \sum_{i=0}^{n-1} \text{IPM}(t_1 + \eta i, t_1 + \eta(i+1)).$$

Therefore, $\forall t_1, t_2 \in [0, 1]$,

$$\frac{\text{IPM}(t_1, t_2)}{t_2 - t_1} \leq \alpha_{\min}.$$

136 On the other hand, we can get $\alpha \geq \alpha_{\min}$ according to the definition of α . In other words, α_{\min} is
 137 the minimum α that meets the conditions of Assumption 3. \square

138 B.1 Generalization bound based on finite samples

139 In this section, we refer to a lemma from [20] to give the finite sample guarantee of Theorem 3.

140 **Lemma 4.** (Sriperumbudur et al. [20]) *Let \mathcal{X} be a measurable space. Suppose k is a universal,*
 141 *measurable kernel such that $\sup_{x \in \mathcal{X}} k(x, x) \leq C$ and \mathcal{H} the reproducing kernel Hilbert space*
 142 *induced by k , with $v := \sup_{x \in \mathcal{X}, f \in \mathcal{H}} \leq \infty$. Then, with \hat{p}, \hat{q} the empirical distributions of p, q from*
 143 *m and n samples, and with probability at least $1 - \xi$, we have,*

$$|\text{IPM}_{\mathcal{H}}(p, q) - \text{IPM}_{\mathcal{H}}(\hat{p}, \hat{q})| \leq \sqrt{18v^2 \log \frac{4}{\xi}} \left(\frac{1}{\sqrt{m}} + \frac{1}{\sqrt{n}} \right). \quad (13)$$

144

145 With Lemma 4 and Theorem 3, we can give the finite sample guarantee for the proposed algorithm
 146 ADMIT.

147 **Theorem 4.** *Suppose we have n i.i.d. sample of units with an empirical measure \hat{p} , and the*
 148 *i th unit received a treatment s_i . Let n_s denote the number of units belonging to $[s, s + \delta]$, and*
 149 $\widehat{\text{IPM}}_{\Delta_{\max}} = \max_{i \in \{1, \dots, n\}} \{\text{IPM}_{\mathcal{G}}(\hat{p}_{\Delta_{s_i}}, \hat{p}_{\Delta_t}^w)\}$. *We assume Assumption 3 holds for a constant α .*
 150 *Then, for a neighborhood size $0 < \delta < 1$, we have,*

$$\epsilon(f_t) \leq \epsilon_w(f_t | T = t) + \widehat{\text{IPM}}_{\Delta_{\max}} + \sqrt{18v^2 \log \frac{4}{\xi}} D_{n_s} + \sigma_{Y_t} + O_p\left(\frac{\alpha}{\sqrt{3n}}\right) + \alpha\delta, \quad (14)$$

151 where $D_{n_s} = \max_{i \in \{1, \dots, n\}} \left\{ \frac{1}{\sqrt{n_{s_i}}} + \frac{1}{\sqrt{n_t}} \right\}$.

152 C Experimental Details

153 C.1 Dataset descriptions

154 **News.** The News dataset, consisting of a random sample of 5,000 news items from the NY Times
 155 corpus [21], was originally introduced as a benchmark for counterfactual inference in the binary
 156 treatment setting [22]. For each news item x , the i th dimension x_i represents the number of
 157 occurrences of the i th word. Following [22, 23], to give meaning to our treatments and outcomes,
 158 we let treatment T and outcome Y^T represent the time readers spending on the news and their
 159 satisfaction with the news, respectively. The same version of the News dataset as DRNet (<https://github.com/d909b/drnet>) is used in this work.
 160

161 **TCGA.** The TCGA project collected gene expression data for various types of cancer from 9,659
 162 individuals, from which we select the 4,000 most variable genes as features to build our dataset as
 163 in [23]. We scaled the features of each patient to have norm 1. To give meaning to our treatments

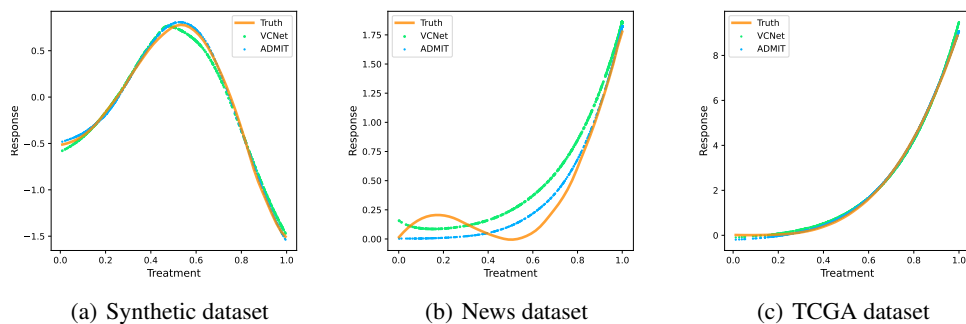


Figure 1: Estimated ADRF on testing set from a typical run of ADMIT and VCNet. The truth is shown in solid orange line.

Table 1: Summary description of datasets.

Dataset	Simulation	News	TCGA
Number of samples	5,000	5,000	9,659
Number of features	6	3,477	4,000

164 and outcomes, we let treatment T and outcome Y^T represent the medication dosage and the risk of
 165 cancer recurrence after receiving corresponding treatment, respectively. The same version of the
 166 TCGA dataset as SCIGAN (<https://github.com/ioanabica/SCIGAN>) is used in this work.

167 A summary description of the datasets is shown in Table 1. We randomly split each dataset into
 168 training set (67%), validation set (23%), and test set (10%). The validation dataset is used for
 169 hyperparameter selection.

170 C.2 Implement details

171 **Baselines.** We implement entropy balancing for continuous treatments (EBCT) [24] using <https://github.com/EddieYang211/ebal-py>, and GPS using Python package "causal-curve" [25]
 172 <https://github.com/ronikobrosly/causal-curve>. Moreover, we use the publicly avail-
 173 able implementation of SCIGAN provided by [23]: <https://github.com/ioanabica/SCIGAN>,
 174 and implementations of VCNet and DRNet provided by [26]: [https://github.com/lushleaf/
 175 varying-coefficient-net-with-functional-tr](https://github.com/lushleaf/varying-coefficient-net-with-functional-tr). We implement our model on PyTorch with
 176 an Nvidia RTX3090 GPU. The implementation of the varying coefficient prediction head we use to
 177 build the inference and re-weighting networks is based on [26], and the kernel we apply in calculating
 178 MMD is the Gaussian kernel based on <https://github.com/oddrose/cfrnet>.
 179

180 **Parameter setting.** We tune parameters based on the validation split of each dataset, and
 181 use the EMSE for evaluation. We tune the following parameters: network learning rate $lr \in$
 182 $\{0.005, 0.001, 0.0005, 0.0003, 0.0001\}$, batch size $bs \in \{100, 200, 500, 1, 000\}$, and neighbour-
 183 hood size $\delta \in \{0.05, 0.1, 0.2\}$. All networks are trained for 200 epochs during tuning.

184 C.3 Dose-response curve

185 To observe the effectiveness of our model visually, the estimated dose-response curves of ADMIT
 186 and VCNet and the truth are plotted in Figure 1. Across different datasets, when the true ADRF is
 187 simpler, both ADMIT and VCNet fit better. Moreover, ADMIT always be able to fit the ADRF better
 188 than VCNet, especially when the true ADRF is relatively complex.

189 References

190 [1] Uri Shalit, Fredrik D Johansson, and David Sontag. Estimating individual treatment effect:
 191 Generalization bounds and algorithms. In *Proceedings of the 34th International Conference on*

- 192 *Machine Learning*, pages 3076–3085. PMLR, 2017.
- 193 [2] Liuyi Yao, Sheng Li, Yaliang Li, Mengdi Huai, Jing Gao, and Aidong Zhang. Representation
194 learning for treatment effect estimation from observational data. In *Proceedings of the 32nd*
195 *Advances in Neural Information Processing Systems*, volume 31, 2018.
- 196 [3] Negar Hassanpour and Russell Greiner. Counterfactual regression with importance sampling
197 weights. In *Proceedings of the 28th International Joint Conference on Artificial Intelligence*,
198 pages 5880–5887, 2019.
- 199 [4] Fredrik D Johansson, Uri Shalit, Nathan Kallus, and David Sontag. Generalization bounds and
200 representation learning for estimation of potential outcomes and causal effects. *arXiv preprint*
201 *arXiv:2001.07426*, 2020.
- 202 [5] Guido W. Imbens and Donald B. Rubin. *Causal Inference for Statistics, Social, and Biomedical*
203 *Sciences: An Introduction*. Cambridge University Press, USA, 2015.
- 204 [6] Paul R Rosenbaum and Donald B Rubin. The central role of the propensity score in observational
205 studies for causal effects. *Biometrika*, 70(1):41–55, 1983.
- 206 [7] Paul R Rosenbaum. Model-based direct adjustment. *Journal of the American statistical*
207 *Association*, 82(398):387–394, 1987.
- 208 [8] Keisuke Hirano and Guido W Imbens. The propensity score with continuous treatments. *Applied*
209 *Bayesian modeling and causal inference from incomplete-data perspectives*, 226164:73–84,
210 2004.
- 211 [9] Yeying Zhu, Donna L Coffman, and Debashis Ghosh. A boosting algorithm for estimating
212 generalized propensity scores with continuous treatments. *Journal of causal inference*, 3(1):25–
213 40, 2015.
- 214 [10] Edward H Kennedy, Zongming Ma, Matthew D McHugh, and Dylan S Small. Non-parametric
215 methods for doubly robust estimation of continuous treatment effects. *Journal of the Royal*
216 *Statistical Society: Series B (Statistical Methodology)*, 79(4):1229–1245, 2017.
- 217 [11] Miguel A Hernán and James M Robins. Causal inference, 2010.
- 218 [12] Sheng Li and Yun Fu. Matching on balanced nonlinear representations for treatment effects
219 estimation. *Advances in Neural Information Processing Systems*, 30, 2017.
- 220 [13] Corinna Cortes and Mehryar Mohri. Domain adaptation and sample bias correction theory and
221 algorithm for regression. *Theoretical Computer Science*, 519:103–126, 2014.
- 222 [14] Baochen Sun, Jiashi Feng, and Kate Saenko. Return of frustratingly easy domain adaptation. In
223 *Proceedings of the 30th AAAI Conference on Artificial Intelligence*, 2016.
- 224 [15] Meijiao Liu, Yicheng Qiang, Weihua Li, Feng Qiu, and An-Chang Shi. Stabilizing the frank-
225 kasper phases via binary blends of ab diblock copolymers. *ACS Macro Letters*, 5(10):1167–1171,
226 2016.
- 227 [16] Yaroslav Ganin, Evgeniya Ustinova, Hana Ajakan, Pascal Germain, Hugo Larochelle, François
228 Laviolette, Mario Marchand, and Victor Lempitsky. Domain-adversarial training of neural
229 networks. *The journal of machine learning research*, 17(1):2096–2030, 2016.
- 230 [17] Hao Wang, Hao He, and Dina Katabi. Continuously indexed domain adaptation. In *Proceedings*
231 *of the 37th International Conference on Machine Learning*, pages 9898–9907. PMLR, 2020.
- 232 [18] Hong Liu, Mingsheng Long, Jianmin Wang, and Yu Wang. Learning to adapt to evolving
233 domains. In *Proceedings of the 34th Advances in Neural Information Processing Systems*,
234 volume 33, pages 22338–22348, 2020.
- 235 [19] Guillermo Ortiz-Jimenez, Mireille El Gheche, Effrosyni Simou, Hermina Petric Maretic, and
236 Pascal Frossard. CDOT: Continuous domain adaptation using optimal transport. *arXiv preprint*
237 *arXiv:1909.11448*, 2019.

- 238 [20] Bharath K Sriperumbudur, Kenji Fukumizu, Arthur Gretton, Bernhard Schölkopf, and Gert RG
239 Lanckriet. On integral probability metrics, ϕ -divergences and binary classification. *arXiv*
240 *preprint arXiv:0901.2698*, 2009.
- 241 [21] David Newman. Bag of words data set. *UCI Machine Learning Respository*, 2008.
- 242 [22] Fredrik Johansson, Uri Shalit, and David Sontag. Learning representations for counterfactual
243 inference. In *Proceedings of the 33rd International conference on machine learning*, pages
244 3020–3029. PMLR, 2016.
- 245 [23] Ioana Bica, James Jordon, and Mihaela van der Schaar. Estimating the effects of continuous-
246 valued interventions using generative adversarial networks. In *Proceedings of the 34th Advances*
247 *in Neural Information Processing Systems*, volume 33, pages 16434–16445, 2020.
- 248 [24] Stefan Tübbicke. Entropy balancing for continuous treatments. *Journal of Econometric Methods*,
249 11(1):71–89, 2022.
- 250 [25] Roni W Kobrosly. causal-curve: A python causal inference package to estimate causal dose-
251 response curves. *Journal of Open Source Software*, 5(52):2523, 2020.
- 252 [26] Lizhen Nie, Mao Ye, Dan Nicolae, et al. VCNet and functional targeted regularization for
253 learning causal effects of continuous treatments. In *Proceedings of the 9th International*
254 *Conference on Learning Representations*, 2020.